Electronic Supplementary Information

Chromium doped Li_2RuO_3 as a positive electrode with superior electrochemical performance for lithium ion batteries

Shengzhou Liu,[a] Jiali Wang,[b] Zixuan Tian,[a] Qian Li,[a] Xiaoqing Tian,[a] Yanhua Cui[b] and Yin Yang*[a]

[a] Institute of Advanced Synthesis, School of Chemistry and Molecular Engineering, Jiangsu National Synergetic Innovation Center for Advanced Materials, Nanjing Tech University, Nanjing 211816, P. R. China.

[b] Institute of Electronic Engineering, China Academy of Engineering Physics, Mianyang, Sichuan, 621000, P. R. China

Corresponding Author:
*Email: ias_yyang@njtech.edu.cn

Experimental Section

Material Synthesis. All the samples, Li_2RuO_3 (LRO) and Cr-doped Li_2RuO_3 ($LiRu_{0.98}Cr_{0.02}O_3$, $LiRu_{0.95}Cr_{0.05}O_3$ and $LiRu_{0.9}Cr_{0.1}O_3$, denoted as LRO-Cr0.02, LRO-Cr0.05 and LRO-Cr0.1, respectively), were synthesized by high-temperature solid-state sintering method. Stoichiometric amounts of Li_2CO_3, Cr_2O_3 and RuO_2 as precursors were mixed using a mortar and pestle for 30 min and then ball milled for 40 min with a 10wt% excess amount of Li_2CO_3 to compensate for Li evaporation during sintering. The resultant mixture were placed in separated alumina crucibles and sintered at 900 °C for 12 hours. The furnace heating rate was set at 2 °C/min and then the furnace was naturally cool to room temperature.

Characterization. X-ray diffraction (XRD) patterns were investigated by Bruker D8 Advance diffractometer equipped with Cu Kα radiation (λ= 0.15406 nm). The morphological features and elemental analysis of the product were characterized by field emission scanning electron microscopy (FESEM) (HITACHI, S-4800). X-ray photoelectron spectroscopy (XPS, Physical Electronics) was employed to check valence state of elements in the samples.

Electrochemical measurements. Type-2025 coin cells were assembled in an argon-filled glovebox. The positive electrodes were fabricated by mixing active material, super-P carbon, and polyvinylidene fluoride binder (PVDF) with weight ratio of 8:1:1. The mixture was pressed onto an Al foil and vacuum dried at 120 °C overnight. A lithium disc was pressed on a thin stainless steel disc as anode. The electrolyte used was 1 M $LiPF_6$ solution in a mixture of ethylene carbonate (EC) and dimethyl carbonate (DMC) with weight ratio of 1:1. Galvanostatic charge-discharge measurements were carried out at room temperature with a battery test system (CT2001A, Wuhan Land Electronics). Cyclic voltammertry (CV) and electrochemical impedance spectroscopy (EIS) measurements of all samples were recorded using CHI 660B. CV was conducted at a scan rate of 0.1 mV s^{-1} in potential window of 2.0-4.6 V and EIS was obtained at 4.2 V during charge process at 1st, 2nd and 30th cycle in the frequency range of 100 kHz to 0.01 Hz.

Table S1. Comparison of electrochemical performance of Cr-doped Li_2RuO_3 with other reported Ru-based layered oxides.

Typical materials	Current density	Voltage range (V)	Initial capacity (mAh g^{-1})	Cycle number	Remaining capacity (mAh/g)	Capacity retention	High rate performance	Ref.
$Li_{2.1}Ru_{0.9}Co_{0.1}O_3$	260 mA g^{-1}	2.0-1.8	275	50	175	64	—	S1
Li_3CoRuO_5	0.1 mA cm^{-2}	2.75-4.2	205	6	180	88%	—	S2
Li_3NiRuO_5	0.1 mA cm^{-2}	2.75-4.2	240	6	160	67%	—	S2
Li_4CoRuO_6	30 mA g^{-1}	2.2-4.2	180	10	130	72%	—	S3
$Li_5Co_{1.5}Ru_{1.5}O_8$	30 mA g^{-1}	2.2-4.2	140	10	115	82%	—	S3
$Li_{1.8}Ru_{0.6}Fe_{0.6}O_3$	0.1 mA cm^{-2}	2.0-4.3	125	7	100	80%	—	S4
$Li_2RuB_{0.15}O_3$	30 mA g^{-1}	2.0-4.6	220	50	210	95%	—	S5
$Li_2Ru_{0.9}Zr_{0.1}O_3$	0.1 mA cm^{-2}	2.8-4.3	205	20	190	93%	—	S6
Li_2RuO_3	16 mA g^{-1}	2.0-4.8	288	40	220	76%	—	S7
$Li_2Mn_{0.4}Ru_{0.6}O_3$	16 mA g^{-1}	2.0-4.8	218	50	165	76%	—	S7
Li_2RuO_3	32 mA g^{-1}	2.0-4.6	280	50	224	80%	—	S8
$Li_2Ru_{0.75}Sn_{0.25}O_3$	32 mA g^{-1}	2.0-4.6	220	50	180	82%	—	S8
$Li_2Ru_{0.75}Ti_{0.25}O_3$	32 mA g^{-1}	2.0-4.6	243	50	175	72%	—	S8
Li_2RuO_3	30 mA g^{-1}	2.0-4.6	260	30	220	85%	—	S9
$Li_{1.23}Ni_{0.155}Ru_{0.615}O_2$	22 mA g^{-1}	2.2-4.3	295	50	210	71%	145 mAh g^{-1} (220 mA g^{-1})	S10
$Li_2Ru_{0.75}Sn_{0.25}O_3$	143 mA g^{-1}	2.0-4.8	180	50	140	78%	107 mAh g^{-1} (458 mA g^{-1})	S11
$Li_2Ru_{0.75}Ti_{0.25}O_3$	143 mA g^{-1}	2.0-4.8	225	50	200	89%	140 mAh g^{-1} (458 mA g^{-1})	S11
$Li_2Ru_{0.6}Mn_{0.4}O_3$	32 mA g^{-1}	2.0-4.6	250	50	200	80%	42 mAh g^{-1} (800 mA g^{-1})	S12
$Li_2Ru_{0.9}Ir_{0.1}O_3$	40 mA g^{-1}	2.0-4.6	200	50	180	90%	82 mAh g^{-1} (800 mA g^{-1})	S13
$Li_2Ru_{0.95}Cr_{0.05}O_3$	32 mA g^{-1}	2.0-4.6	298	50	262	88%	179 mAh g^{-1} (800 mA g^{-1})	TW*
$Li_2Ru_{0.95}Cr_{0.05}O_3$	160 mA g^{-1}	2.0-4.2	253	120	220	87%	—	TW*

TW*: This Work

Table S2. Fitting values of R_f and R_{ct} of $Li_2Ru_xCr_{1-x}O_3$ (x=0, 0.02, 0.05, 0.1) series.

x value	0		0.02		0.05		0.1	
State	R_f (Ω)	R_{ct} (Ω)	R_f (Ω)	R_{ct} (Ω)	R_f (Ω)	R_{ct} (Ω)	R_f (Ω)	R_{ct} (Ω)
Pristine	24.34	76.73	24.15	32.42	14.28	29	51.75	123.4
2nd	41.56	130	40.24	73.43	40.01	64.56	45.92	85.34
30th	9.68	231.3	6.088	156.9	5.59	127.1	8.816	132.8

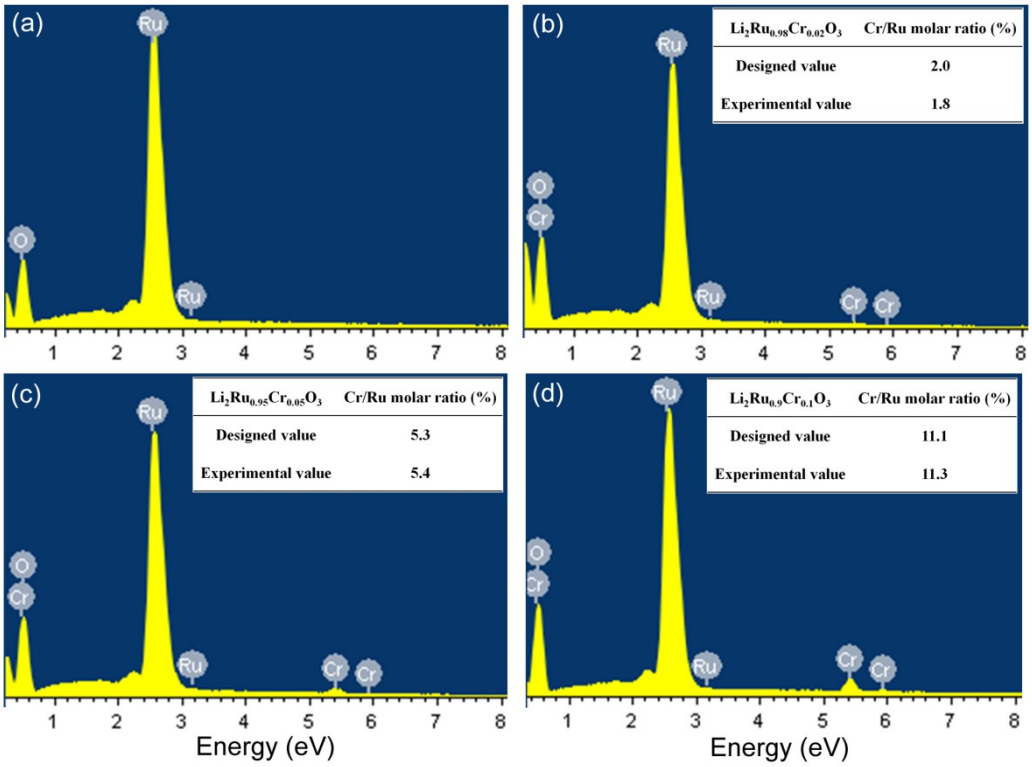

Fig. S1 EDS spectra of $LiRu_{1-x}Cr_xO_3$ series with (a) x=0; (b) x=0.02; (c) x=0.05 and (d) x=0.1. The inset tables show the designed and experimental values for molar ratio of Cr/Ru.

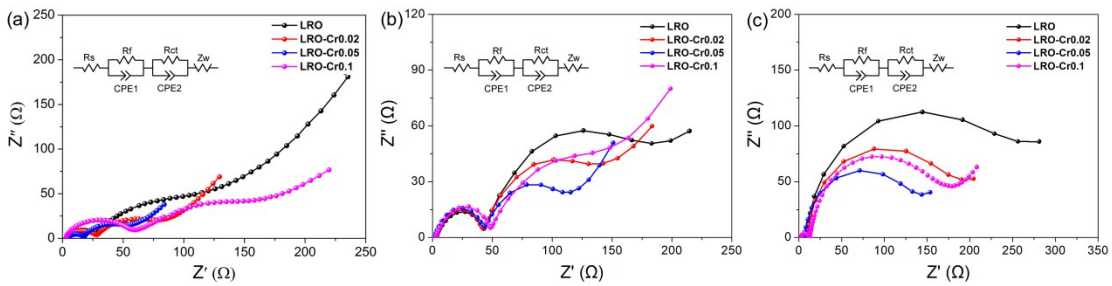

Fig. S2 EIS plots of $LiRu_{1-x}Cr_xO_3$ (x=0, 0.02, 0.05, 0.1) series at (a) the initial cycle; (b) 2nd cycle and (c) 30th cycle.

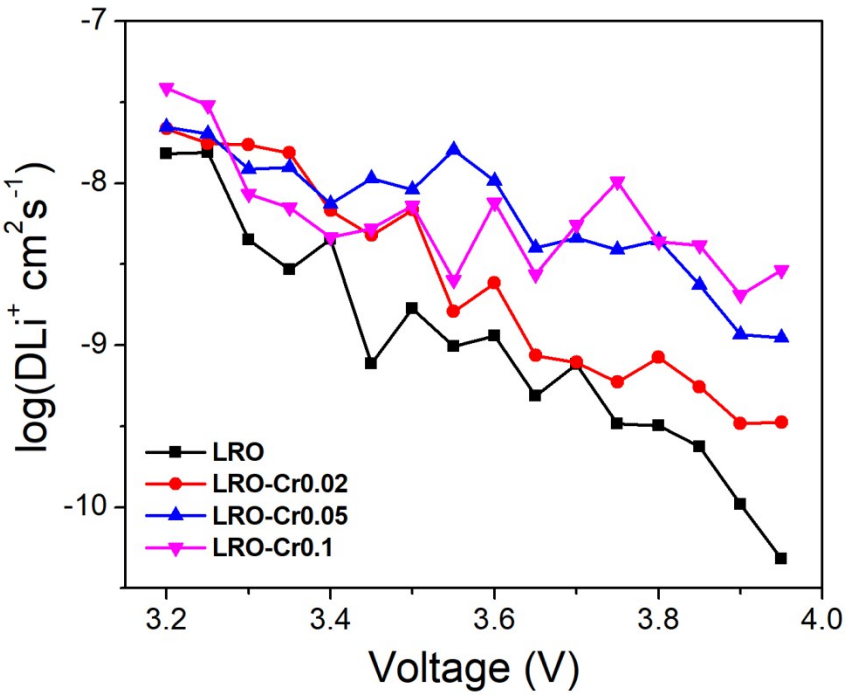

Fig. S3 The chemical diffusion coefficients of Li^+ for $Li_2Ru_xCr_{1-x}O_3$ (x=0, 0.02, 0.05, 0.1) series at different state of charge from EIS.

References

S1. P. Arunkumar, W. J. Jeong, S. Won and W. B. Im, *Journal Of Power Sources*, 2016, **324**, 428-438.

S2. S. Laha, E. Moran, R. Saez-Puche, M. A. Alario-Franco, A. J. Dos Santos-Garcia, E. Gonzalo, A. Kuhn, S. Natarajan, J. Gopalakrishnan and F. Garcia-Alvarado, *J Mater Chem A*, 2013, **1**, 10686-10692.

S3. S. Tamilarasan, D. Mukherjee, S. Sampath, S. Natarajan and J. Gopalakrishnan, *Solid State Ionics*, 2016, **297**, 49-58.

S4. H. Kobayashi, R. Kanno, M. Tabuchi, H. Kageyama, O. Nakamura and M. Takano, *Journal Of Power Sources*, 1997, **68**, 686-691.

S5. B. Li, H. J. Yan, Y. X. Zuo and D. G. Xia, *Chem Mater*, 2017, **29**, 2811-2818.

S6. G. J. Moore, C. S. Johnson and M. M. Thackeray, *Journal Of Power Sources*, 2003, **119**, 216-220.

S7. D. Mori, H. Kobayashi, T. Okumura and Y. Inaguma, *Electrochemistry*, 2015, **83**, 1071-1076.

S8. M. Sathiya, A. M. Abakumov, D. Foix, G. Rousse, K. Ramesha, M. Saubanere, M. L. Doublet, H. Vezin, C. P. Laisa, A. S. Prakash, D. Gonbeau, G. VanTendeloo and J. M. Tarascon, *Nat Mater*, 2015, **14**, 230-238.

S9. B. A. Li, R. W. Shao, H. J. Yan, L. An, B. Zhang, H. Wei, J. Ma, D. G. Xia and X. D. Han, *Adv Funct Mater*, 2016, **26**, 1330-1337.

S10. X. B. Wang, W. F. Huang, S. Tao, H. Xie, C. Q. Wu, Z. Yu, X. Z. Su, J. X. Qi, Z. U. Rehman, L. Song, G. B. Zhang, W. S. Chu and S. Q. Wei, *Journal Of Power Sources*, 2017, **359**, 270-276.

S11. A. K. Kalathil, P. Arunkumar, D. H. Kim, J. W. Lee and W. B. Im, *Acs Appl Mater Inter*, 2015, **7**, 7118-7128.

S12. M. Sathiya, K. Ramesha, G. Rousse, D. Foix, D. Gonbeau, A. S. Prakash, M. L. Doublet, K. Hemalatha and J. M. Tarascon, *Chem Mater*, 2013, **25**, 1121-1131.

S13. S. Sarkar, P. Mahale and S. Mitra, *J Electrochem Soc*, 2014, **161**, A934-A942.